Inorg. Chem. **2006**, *45*, 362–369

Static and Dynamic Quenching of Ru(II) Polypyridyl Excited States by Iodide

Andras Marton, Christopher C. Clark, Ramya Srinivasan, Robert E. Freundlich, Amy A. Narducci Sarjeant, and Gerald J. Meyer*

Departments of Chemistry and Materials Science and Engineering, Johns Hopkins University, Baltimore, Maryland 21218

Received August 26, 2005

The metal-to-ligand charge-transfer (MLCT) excited states of $Ru(bpy)_2(deeb)(PF_6)_2$, where bpy is 2,2-bipyridine and deeb is 4,4′-$(CO_2CH_2CH_3)_2$-2,2′-bipyridine, in dichloromethane were found to be efficiently quenched by iodide at room temperature. The ionic strength dependence of the UV–visible absorption spectra gave evidence for ion pairing. Iodide was found to quench the excited states by static and dynamic mechanisms. Stern–Volmer and Benesi–Hildebrand analysis of the spectral data provided a self-consistent estimate of the iodide–$Ru(bpy)_2(deeb)^{2+}$ adduct in dichloromethane, $K = 59\,700\ M^{-1}$. Transient absorption studies clearly demonstrated an electron-transfer quenching mechanism with transient formation of $I_2^{\bullet-}$ in high yield, $\phi = 0.25$ for 355 or 532 nm excitation. For $Ru(bpy)_2(deeb)(PF_6)_2$ in acetonitrile, similar behavior could be observed at higher iodide concentrations than that required in dichloromethane. The parent $Ru(bpy)_3^{2+}$ compound also ion pairs with iodide in CH_2Cl_2, and light excitation gave a higher $I_2^{\bullet-}$ yield, $\phi = 0.50$. X-ray crystallographic, IR, and Raman data gave evidence for interactions between iodide and the coordinated deeb ligand in the solid state.

Introduction

Photoinduced charge-transfer processes in transition metal complexes are of significant importance in dye-sensitized solar cells (DSSC) that are presently receiving widespread attention as a potentially cost-effective alternative to silicon-based photovoltaics.[1−3] The DSSCs function by a mechanism in which a photoexcited Ru(II) polypyridyl compound injects an electron into a TiO_2 nanoparticle.[2,3] In the most efficient DSSCs, the Ru(II) state is regenerated by I^-, present in an external electrolyte at high (∼0.45 M) concentrations. The oxidized iodide products are subsequently reduced at a Pt counter electrode. The DSSC is thus termed regenerative as no net chemical products are formed. Although the interfacial electron-transfer processes at sensitized semiconductors have been studied extensively, much less is known about the interaction between the Ru(II) polypyridyl compounds and supporting electrolytes that contain iodide.[4−7]

Previously, we communicated experimental conditions under which Ru(II) polypyridyl metal-to-ligand charge-transfer (MLCT) excited states effectively oxidize iodide.[4] Ion-pairing interactions between I^- and $Ru(bpy)_3^{2+}$ or $Ru(bpy)_2(deeb)^{2+}$, where bpy = 2,2-bipyridine and deeb = 4,4′-$(CO_2CH_2CH_3)_2$-2,2′-bipyridine, greatly facilitated excited-state iodide oxidation in dichloromethane and, to a lesser extent, in acetonitrile. To our knowledge, it was the first example of efficient MLCT excited-state quenching by iodide.[8,9] Herein, we provide further evidence for ion pairing and new mechanistic details of excited-state electron transfer.

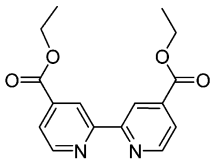

4,4'-$(CO_2CH_2CH_3)_2$-2,2'bipyridine

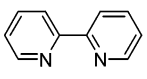

2,2-bipyridine

* Author to whom correspondence should be addressed. E-mail: meyer@jhu.edu.

(1) O'Regan, B.; Gratzel, M. *Nature* **1991**, *353*(6346), 737−740.
(2) Gratzel, M. *Nature* **2001**, *414*(6861), 338−344.
(3) Watson, D. F.; Meyer, G. J. *Annu. Rev. Phys. Chem.* **2005**, *56*, 119−156.
(4) Clark, C. C.; Marton, A.; Meyer, G. J. *Inorg. Chem.* **2005**, *44*(10), 3383−3385.
(5) Pelet, S.; Moser, J. E.; Gratzel, M. *J. Phys. Chem. B* **2000**, *104*(8), 1791−1795.
(6) Nasr, C.; Hotchandani, S.; Kamat, P. V. *J. Phys. Chem. B* **1998**, *102*(25), 4944−4951.
(7) Fitzmaurice, D. J.; Frei, H. *Langmuir* **1991**, *7*(6), 1129−1137.
(8) Birks, J. B. *Photophysics of Aromatic Molecules*; Wiley-Interscience: London, 1970.
(9) Maestri, M.; Bolletta, F.; Moggi, L.; Balzani, V.; Henry, M. S.; Hoffman, M. Z. *J. Chem. Soc., Chem. Commun.* **1977**, (14), 491−492.

10.1021/ic051467j CCC: $33.50
Published on Web 12/10/2005

In addition, X-ray crystallographic, IR, and Raman data gave evidence for electronic interactions between iodide and the coordinated deeb ligand of $Ru(bpy)_2(deeb)^{2+}$ in the solid state.

Experimental Section

Materials. Tetrabutylammonium iodide (Sigma Aldrich), tetrabutylammonium hexafluorophosphate (Fluka), tetrabutylammonium tri-iodide (Fluka), dichloromethane (HPLC grade, EMD), acetonitrile (Burdick and Jackson), and ethyl ether (Fischer) were all used as received. Samples of $Ru(bpy)_2(deeb)(PF_6)_2$ and $Ru(bpy)_3(PF_6)_2$ were available from previous studies.[4]

Spectroscopy. Photoluminescense. Steady-state photoluminescence (PL) spectra were obtained with a Spex Fluorolog that had been calibrated with a certified lamp. Samples of $Ru(bpy)_2(deeb)(PF_6)_2$ and $Ru(bpy)_3(PF_6)_2$ in dichloromethane and acetonitrile were purged with N_2 gas for 20 min. PL spectra were taken with 500 nm excitation. For comparative iodide studies, all intensities were corrected for absorption changes at the excitation wavelength. Time-resolved PL data were obtained with the same setup as that for the transient absorption experiments (see below).

UV−Vis Absorbance. All UV−visible absorption data were obtained on a Varian Cary 50 UV−vis spectrophotometer in a 1-cm^2 quartz cuvette at room temperature.

Transient Absorbance. Transient absorption spectra were obtained as described earlier.[10] In short, pulsed 532.5-nm light (8−10 ns fwhm, 2.5 mJ/pulse) from a Surelite II Nd:YAG, Q-switched laser was used as the excitation source. A homogeneous portion of the laser was selected using an iris and then expanded to approximately 1 cm^2 using a quartz concave lens. A sample was probed at a right angle using a 150 W pulsed Xe lamp (Applied Photophysics). Each kinetic trace was acquired by averaging 40−200 laser shots at 1 Hz repetition rate. Samples were prepared in a 1-cm^2 quartz cuvette and purged with nitrogen gas for 20 min. Extreme precautions were taken not to introduce any impurity during the preparation and degassing process. A change in volume due to purging was accounted for by taking the absorption spectra before and after degassing.

IR. Infrared spectra of all samples were acquired on a Nexus 670 FT-IR with a Smart Golden Gate attenuated total reflectance (ATR) accessory from Thermo Nicolet. Samples were acquired at 1, 2, and 4 cm^{-1} resolutions. At the highest resolution, sharp peaks from the diamond ATR accessory were observed, which could not be fully subtracted. For this reason, the data presented here were obtained at 4 cm^{-1} resolution.

Raman. FT-Raman spectra were obtained with the Raman module of a Nexus 670 FT-IR equipped with a Nd:YAG laser (1064 nm) and a liquid nitrogen-cooled InGaAs detector. Spectra were an average of 256 scans collected at 1 cm^{-1} resolution. A laser power of 1 W was used.

X-ray Crystallography. Crystals of $Ru(bpy)_2(deeb)(I)_2$ were grown by the addition of a 10-fold molar excess of tetrabutylammonium iodide to $Ru(bpy)_2(deeb)(PF_6)_2$ in acetonitrile. The solution was placed in an opened vial inside a diethyl ether vapor-filled chamber. Dark red-orange crystals formed within 3 days. A suitable crystal of $Ru(bpy)_2(deeb)(I)_2$ was mounted in oil on the end of a glass fiber and used for X-ray crystallographic analysis. The X-ray intensity data were measured at 110 K on an Oxford Diffraction Xcalibur3 system equipped with a graphite monochromator and a CCD detector. The final cell was obtained through a refinement of 6664 reflections to a maximum resolution of 0.67 Å. Data were collected via a series of 1.0° φ and ω scans.

The frames were integrated with the Oxford Diffraction *CrysAlisRED* software package. A face-indexed absorption correction and an interframe scaling correction were also applied. The structure was solved using direct methods and refined using the Bruker *SHELXTL* (v6.1) software package. Analysis of the data showed no sample decomposition.

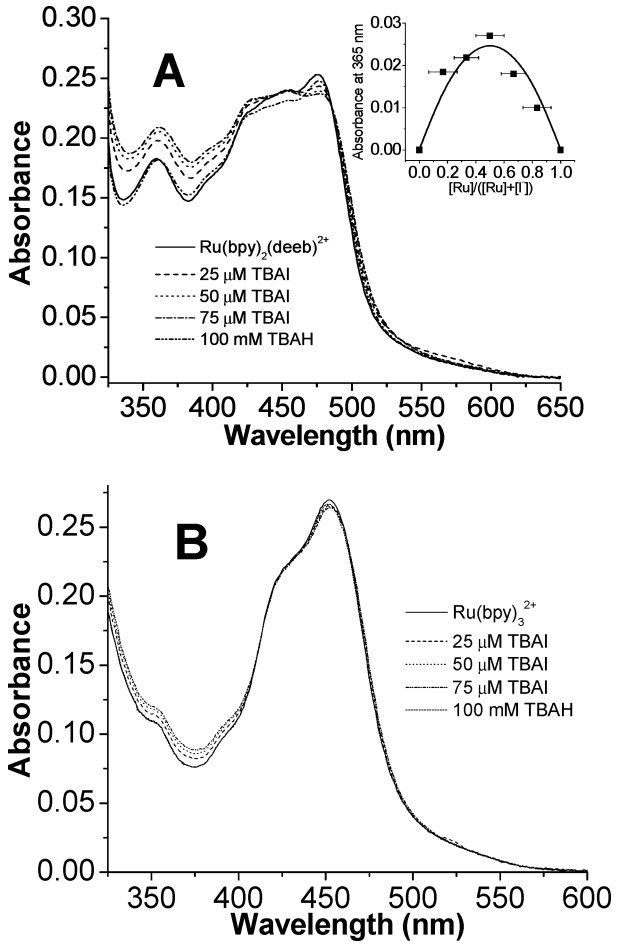

Figure 1. Room-temperature UV−visible absorption spectra of (A) $Ru(bpy)_2(deeb)(PF_6)_2$ and (B) $Ru(bpy)_3(PF_6)_2$ in dichloromethane with a trace of triethylamine and with the indicated tetrabutylammonium iodide (TBAI) concentrations. A final spectrum with 100 mM tetrabutylammonium hexafluorophosphate (TBAH) added is also shown. (Inset) Job plot with data obtained at 365 nm.

Results

Figure 1 shows the absorption spectra of $Ru(bpy)_2(deeb)(PF_6)_2$ and $Ru(bpy)_3(PF_6)_2$ in CH_2Cl_2. For the heteroleptic $Ru(bpy)_2(deeb)^{2+}$, the Ru → bpy and Ru → deeb MLCT bands are not well resolved, but Ru → deeb charge transfer accounts for most of the oscillator strength at lower energies (λ > 480 nm). The addition of tetrabutylammonium iodide (TBAI) resulted in distinct spectral changes. A decrease in intensity of the Ru → deeb MLCT absorption band was observed as well as a red-shift of the spectra, Figure 1A. In addition, an increase in intensity was seen between 325 and ∼425 nm. Job plots (see Figure 1A, inset) and the presence of isosbestic points in the absorption spectra reveal a 1:1 stoichiometry of iodide to ruthenium compound up to

(10) Argazzi, R.; Bignozzi, C. A.; Heimer, T. A.; Castellano, F. N.; Meyer, G. J. *Inorg. Chem.* **1994**, *33*(25), 5741−5749.

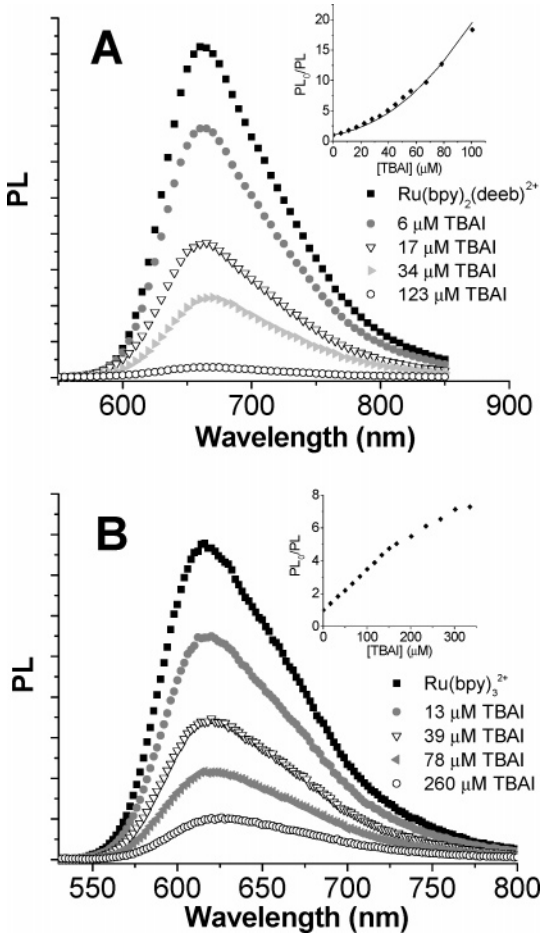

Figure 2. Room-temperature photoluminescence spectra of (A) $Ru(bpy)_2(deeb)^{2+*}$ and (B) $Ru(bpy)_3^{2+*}$ in dichloromethane with the indicated concentrations of tetrabutylammonium iodide (TBAI). (Insets) Fractional PL quenching as a factor of TBAI concentration.

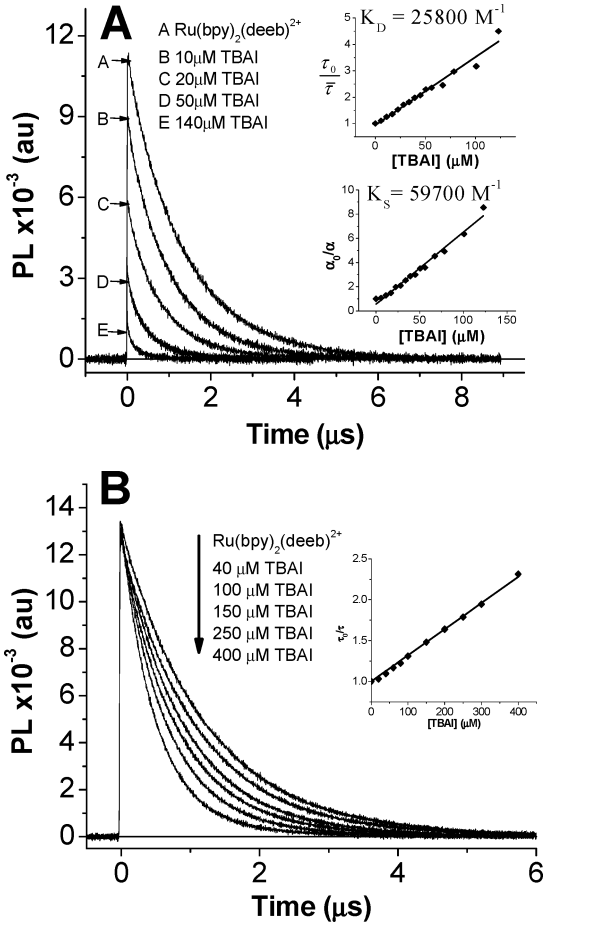

Figure 3. Room-temperature time-resolved PL decays of $Ru(bpy)_2(deeb)^{2+*}$ in (A) neat dichloromethane and (B) 100 mM tetrabutylammonium hexafluorophosphate at the indicated terabutylammonium iodide (TBAI) concentrations. The samples were excited with 532 nm light (~3 mJ/pulse), and the PL was monitored at 650 nm. (Inset) (A) Fractional average lifetime and initial amplitude quenching as a function of TBAI concentration and (B) fractional lifetime quenching.

concentrations of 50 μM.[11] The isosbestic points were lost at higher iodide concentrations. $Ru(bpy)_3^{2+}$ also showed these spectral changes, but the magnitude was smaller precluding an accurate Job analysis, Figure 1B. These effects were also observed for $[Ru(bpy)_2(deeb)](PF_6)_2$ in acetonitrile, but the iodide concentration had to be increased by about 2 orders of magnitude.

The UV−vis spectral changes induced by iodide could largely be reversed with the addition of 100 mM tetrabutylammonium hexafluorophosphate (TBAH), Figure 1. In some cases, the absorption at ~365 nm did not decrease to the initial value. This behavior was particularly evident when the solution was irradiated for prolonged times and was thought to be due to the formation of tri-iodide, I_3^-. Consistent with this hypothesis, the addition of triethylamine to the solution was found to decrease the absorption at 365 nm to the initial value. Subtraction of the absorption spectrum of $Ru(bpy)_2(deeb)^{2+}$ in CH_2Cl_2 from the spectrum of $Ru(bpy)_2(deeb)^{2+}$ with 100 mM iodide indicated the existence of two absorption bands with $\lambda_{max} = 375$ and 501 nm. The same analysis for $Ru(bpy)_3^{2+}$ gave a similar spectrum with $\lambda_{max} = 365$ and 472 nm.

(11) Job, P. *Ann. Chim. Appl.* **1928**, *9*, 113−203.

The steady-state photoluminescence (PL) intensity from $Ru(bpy)_2(deeb)^{2+*}$ and $Ru(bpy)_3^{2+*}$ in dichloromethane was quenched by the addition of iodide, Figure 2. Normalized spectra for the quenching of $Ru(bpy)_2(deeb)^{2+*}$ show that the relative intensity on the high-energy side of the spectra was enhanced. The full-width at half-maximum was found to increase by 670 cm^{-1} when the iodide concentration was increased to 80 μM. The Stern−Volmer plot of the quenching data for $Ru(bpy)_2(deeb)^{2+}$ was upward curving, Figure 2A, inset.

Time-resolved PL studies of $Ru(bpy)_2(deeb)^{2+*}$ revealed that both the initial amplitude and the lifetime were quenched by iodide, Figure 3A. Both processes were well described by the Stern−Volmer model from which equilibrium and quenching constants were abstracted.[12] In 100 mM TBAH, the static component was completely absent with purely dynamic iodide quenching, Figure 3B. At lower TBAH concentrations, the static component could be observed. The Stern−Volmer analyses of data obtained at four different TBAH concentrations are summarized in Table 1. For Ru-

(12) Lakowicz, J. R. *Principles of Fluorescence Spectroscopy*, 2nd ed.; Kluwer Academic/Plenum Publishers: New York, 1999.

Table 1. Stern−Volmer Quenching Constants for $Ru(bpy)_2(deeb)^{2+*}$ by Iodide as a Function of Ionic Strength

[TBAH], mM	K_s, M^{-1}	K_D, M^{-1}
0	59700 ± 2100	25800 ± 1200[a]
1	2200 ± 60	12600 ± 110[a]
10	150 ± 25	8000 ± 100
100	n/a	3200 ± 40

[a] Average lifetimes were obtained by eq 2.

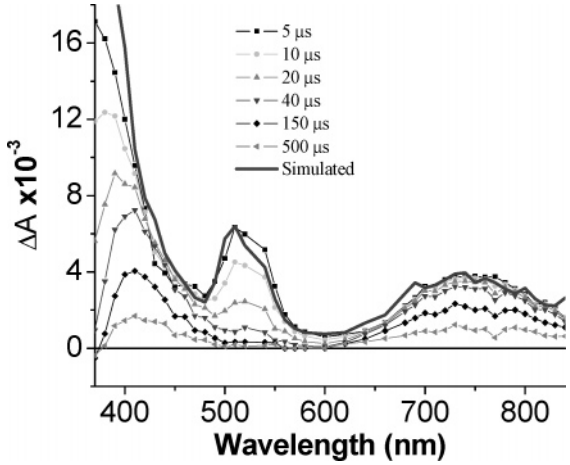

Figure 4. Time-resolved absorption difference spectra observed at the indicated delay times after pulsed-light excitation (532 nm, 8−10 ns fwhm, 2 mJ/pulse) of 15 μM of $Ru(bpy)_2^{2+}$(deeb) and 10 mM of TBAI in dichloromethane at room temperature. Overlaid is a simulated spectrum based on a 1:1 stoichiometry of $I_2^{\bullet-}$/$Ru(bpy)_2(deeb^-)^+$.

$(bpy)_3^{2+*}$, static quenching was observed at low iodide but saturated when the $[I^-]/[Ru(bpy)_3^{2+}]$ ratio was greater than 1.6:1. This saturation could also be seen in Stern−Volmer plots of the steady-state data, Figure 2B, inset.

Excited-state decay was nonexponential in dichloromethane solutions with iodide. These time-resolved data were well described by a biexponential kinetic model, eq 1. An average lifetime was calculated as the first moment, eq 2.[12]

$$PLI(t) = \sum_{i=1}^{2} \alpha_i \exp[-(t/\tau_i)] \quad (1)$$

$$\bar{\tau} = \frac{\sum_{i=1}^{2} \alpha_i \tau_i^2}{\sum_{i=1}^{2} \alpha_i \tau_i} \quad (2)$$

Excited-state decays measured in 10 and 100 mM TBAH/CH_2Cl_2 were well described by a first-order kinetic model at all iodide concentrations.

Nanosecond transient absorption studies with pulsed green-light excitation of 15 μM of $Ru(bpy)_2(deeb)^{2+}$ with 10 mM of TBAI in dichloromethane are shown in Figure 4. The absorption band observed at 530 nm was assigned to $Ru(bpy)_2(deeb^-)^+$, and those at 410 and 750 nm are characteristic for $I_2^{\bullet-}$.[13] Simulations based on 1:1 concentrations of the absorption spectra of $Ru(bpy)_2(deeb^-)^+$ and the spectrum of $I_2^{\bullet-}$ obtained by photodecomposition of tri-iodide in dichloromethane are overlaid on the observed spectra.[13] The quantum yield for production of these charge-separated states was determined to be $\phi = 0.25 \pm 0.04$ by nanosecond actinometry with 355 or 532 nm light excitation.[14] Similar transient features were observed after pulsed excitation of $Ru(bpy)_3^{2+}$ and TBAI dichloromethane solutions, consistent with the photogeneration of $Ru(bpy)_2(bpy^-)^+$ and $I_2^{\bullet-}$. With $Ru(bpy)_3^{2+}$, the cage-escape yields were higher, $\phi = 0.50 \pm 0.06$. For both compounds, the formation of $I_2^{\bullet-}$ was within the instrument response time, consistent with rapid excited-state electron transfer, $k_{et} > 10^8$ s^{-1}.

Table 2. Crystal Parameters for $Ru(bpy)_2(deeb)(I)_2$ and $Ru(bpy)_2(deeb)(PF_6)_2$

	$Ru(bpy)_2(deeb)(I)_2$	$Ru(bpy)_2(deeb)(PF_6)_2$
empirical formula	C36 H32 I2 N6 O5 Ru	C36 H32 F12 N6 O4 P2 Ru
fw	983.55	1003.69
cryst color, habit	red-orange, blade	red-orange, blade
temp	110 K	110 K
radiation	Mo Kα (λ = 0.71073 Å)	Mo Kα (λ = 0.71073 Å)
space group	*P*2(1)/*c*	*P*2(1)/*c*
unit cell dimensions	a = 11.9326(10) Å α = 90° b = 23.378(2) Å β = 102.829(9)° c = 13.2564(16) Å γ = 90° V = 3605.7(6) Å^3	a = 12.0351(11) Å α = 90° b = 23.6776(14) Å β = 100.262(8)° c = 13.7825(14) Å γ = 90° V = 3864.7(6) Å^3
Z	4	4
calcd density	1.812 Mg/m^3	1.725 Mg/m^3
abs coeff	2.19829 mm^{-1}	0.59612 mm^{-1}
$R(F)$%	0.0826	0.0958
$R(wF^2)$%	0.1684	0.1353

The disappearance of $Ru(bpy)_2(deeb^-)^+$ followed a first-order kinetic model with a rate constant that was independent of the excitation irradiance, $k = 1.15 \times 10^5$ s^{-1}. The $Ru(bpy)_2(deeb^-)^+$ lifetime was sensitive to the tetrabutylammonium tri-iodide ($TBAI_3$) concentration and decreased linearly with increasing $[TBAI_3]$, $k = 2.2 \times 10^{10}$ M^{-1} s^{-1}. The $I_2^{\bullet-}$ concentration decreased with second-order kinetics, 7×10^9 M^{-1} s^{-1}. The loss of both $Ru(bpy)_2(deeb^-)^+$ and $I_2^{\bullet-}$ occurred without any new absorption bands in the 400−800 nm region. UV−vis absorption spectra, recorded before and after transient absorption experiments, showed no changed in the visible region, but an increase in the I_3^- concentration (<2.5 μM) was often noted.

The iodide and PF_6^- salts of $Ru(bpy)_2(deeb)^{2+}$ were X-ray crystallographically characterized, Table 2. Space-filling models are shown in Figure 5. The two iodide anions were located above the ester groups of the deeb ligand and were 3.83 and 3.97 Å away from the carbonyl carbon atoms. The interionic iodide−iodide distance was 6.23 Å. In contrast, the PF_6^- salt had the two anions closest to opposite bpy ligands. The angle between the ester group and the pyridine plane was found to be smaller for the iodide salt but within the range found for those of other crystallographically characterized transition metal compounds with a coordinated deeb ligand(s).[15−18]

(13) Devonshire R.; Weiss, J. J. *J. Phys. Chem.* **1968**, *72*(11), 3815−3820.

(14) Yoshimura, A.; Hoffman, M. Z.; Sun, H. *J. Photochem. Photobiol., A* **1993**, *70*(1), 29−33.

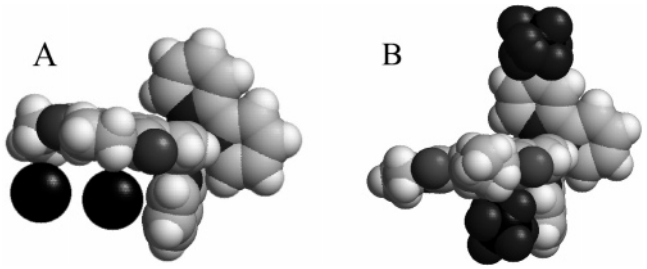

Figure 5. Space-filling model from the crystal structures of (A) Ru(bpy)$_2$(deeb)(I)$_2$ and (B) Ru(bpy)$_2$(deeb)(PF$_6$)$_2$.

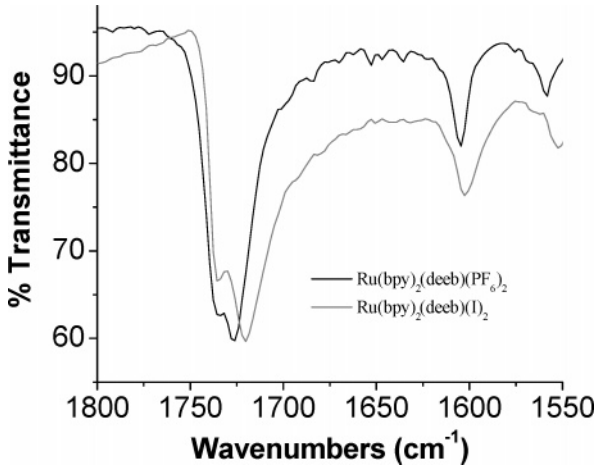

Figure 6. FT-IR spectra of the I$^-$ and PF$_6^-$ crystals of Ru(bpy)$_2$(deeb)$^{2+}$.

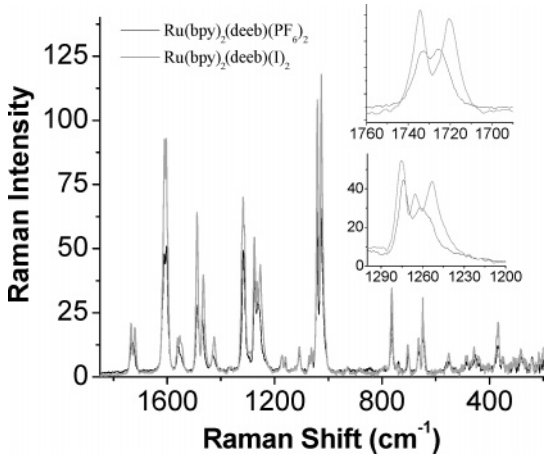

Figure 7. FT-Raman spectra of the I$^-$ and PF$_6^-$ crystals of Ru(bpy)$_2$(deeb)$^{2+}$.

Figures 6 and 7 show the IR and Raman spectra of the I$^-$ and PF$_6^-$ salts. In both spectra, there was a clear change in the carbonyl vibration frequency. The asymmetric ν(CO) stretch at ~1730 cm^{-1} shows two overlapping bands, consistent with the two different ester environments observed in the crystal structures. Interestingly, the higher-energy band is observed at about the same frequency for both salts. The lower-energy band, on the other hand, appears 7 cm^{-1} (2.5 cm^{-1}) lower in energy in the IR (Raman) spectra of the iodide salt. Raman spectroscopy also reveals subtle but significant changes in the bipyridine vibration modes observed in the 1290−1230 cm^{-1} region.

Discussion

Strong evidence for the presence of ground-state adducts between Ru(II) polypyridyl compounds and iodide were found both in dichloromethane solution and in the solid state. These findings are in good agreement with our previous communication[4] and generally support the notion raised by others that related ion pairing occurs at sensitized metal−oxide interfaces.[5−7,19] A Job analysis of the Ru(bpy)$_2$(deeb)$^{2+}$ absorption data reveals a 1:1 Ru(II)/I$^-$ stoichiometry at ~50 μM concentrations. At higher iodide concentrations, isosbestic points were lost, and a 1:2 Ru(II)/I$^-$ stoichiometry was assumed. Below, we discuss ion pairing in the solid state and solution as well as mechanistic details of iodide photooxidation by these MLCT excited states.

Solid-State Ion Pairing. The crystallographic data show that the two iodide counterions are associated with a single deeb ligand in Ru(bpy)$_2$(deeb)$^{2+}$. The interionic distance between the iodides is 6.246(1) Å, and the iodides are I1−C31 = 3.974(9) Å and I2−C34 = 3.835(11) Å away from the carbonyl carbons of the ester groups. On the basis of electrostatic considerations, one might have expected the two anions to be spatially situated farther apart, as was observed for the PF$_6^-$ ions in the crystal structure of Ru(bpy)$_2$(deeb)(PF$_6$)$_2$.

Elliott and Walters have reported crystallographic evidence for ion pairing between iodide and Cr(4,4′-(CH$_3$)$_2$-bpy)$_2$(NSC)$_2^+$.[19] The iodide was found to be situated 3.607 Å above the plane of one of the diimine ligands. They postulated that iodide charge transfer was to the π* orbitals of the diimine ligand. Iodide is well-known to form similar charge-transfer adducts with aromatic hydrocarbons.[20,21] For Ru(bpy)$_2$(deeb)(I)$_2$, the iodide ions are offset from the plane of the pyridines. The iodides interact most directly with the ester functional groups. This interaction is evident in the vibrational data, with measurable shifts in the asymmetric CO stretch relative to the PF$_6^-$ salt. Consistent with the structural data, very subtle spectroscopic changes were observed in the bipyridine framework stretching region between 1290 and 1230 cm^{-1}.

The dihedral angles between the plane of a pyridine ring and the line defined by the C═O bond of the corresponding ester group differ in the PF$_6^-$ and I$^-$ crystal structures. The ester groups in the iodide salt are in a more coplanar arrangement with the bipyridine rings by 7 and 4°. Although the effect is small, such a structural change has theoretically been shown to influence the overlap of the pyridine and carbonyl π orbitals.[22] This geometric change could account

(15) Kinnunen, T. J. J.; Haukka, M.; Pakkanen, T. A. *J. Organomet. Chem.* **2002**, *654*(1−2), 8−15.
(16) Chen, C. T.; Liao, S. Y.; Lin, K. J.; Chen, C. H.; Lin, T. Y. J. *Inorg. Chem.* **1999**, *38*(11), 2734−2741.
(17) Xue, W. M.; Chan, M. C. W.; Su, Z. M.; Cheung, K. K.; Liu, S. T.; Che, C. M. *Organometallics* **1998**, *17*, 7(8), 1622−1630.
(18) Shklover, V.; Nazeeruddin, M. K.; Zakeeruddin, S. M.; Barbe, C.; Kay, A.; Haibach, T.; Steurer, W.; Hermann, R.; Nissen, H. U.; Gratzel, M. *Chem. Mater.* **1997**, *9*(2), 430−439.
(19) Walter, B. J.; Elliott, C. M. *Inorg. Chem.* **2001**, *40*(23), 5924−5927.
(20) Bockman, T. M.; Chang, H. R.; Drickamer, H. G.; Kochi, J. K. *J. Phys. Chem.* **1990**, *94*(22), 8483−8493.
(21) Benesi, H. A.; Hildebrand, J. H. *J. Am. Chem. Soc.* **1949**, *71*(8), 2703−2707.

for the red-shift of the $Ru(bpy)_2(deeb)^{2+}$ MLCT absorption observed in concentrated iodide solutions. We emphasize that although this dihedral angle is significantly different for the two structures characterized herein, both are within the range reported for other transition metal compounds with coordinated deeb or dcb ligands, where dcb is 4,4′-$(CO_2H)_2$-2,2′-bipyridine.[15−18]

Solution Ion Pairing. The static component observed in the time-resolved photoluminescence quenching with iodide provides direct evidence for adduct formation between the Ru(II) compounds and iodide in dichloromethane solutions. The number of excited states created with light excitation decreased with increased iodide concentration. These intensity decreases cannot be explained by ground-state absorption changes and are a classic signature for the presence of ground-state adducts.[12] A standard Stern−Volmer analysis of this static component for $Ru(bpy)_2(deeb)^{2+*}$ directly yields the equilibrium constant $K_S = 59\ 700\ M^{-1}$ for the equilibrium depicted in eq 3. The lifetime data yields a quenching rate constant of $k_q = 1.9 \times 10^{10}\ M^{-1}\ s^{-1}$.

$$Ru(bpy)_2(deeb)^{2+} + I^- \rightleftharpoons [Ru(bpy)_2(deeb),I]^+ \qquad (3)$$

The upward curvature in the steady-state photoluminescence quenching data was also indicative, but not required, for static quenching.[12,23] A system exhibiting both static and dynamic quenching can be described by eq 4:

$$\frac{PL_0}{PL} = 1 + (K_D + K_S)[I^-] + K_D K_S [I^-]^2 \qquad (4)$$

where $[I^-]$ is the free iodide concentration and K_D and K_S are the dynamic and static quenching constants, respectively.[12,23] To calculate the free iodide concentration, eq 5 was solved for *x*, which was then subtracted from the initial (i.e., added) iodide concentration, $[I^-]_0$, to calculate $[I^-]$.

$$K_D = \frac{x}{([Ru(bpy)_2(deeb)^{2+}]_0 - x) \times ([I^-]_0 - x)} \qquad (5)$$

With this approach and the Stern−Volmer constants measured from the time-resolved PL data, the steady-state quenching of $Ru(bpy)_2(deeb)^{2+}$ by iodide in dichloromethane was accurately modeled, Figure 2A, inset.

The spectral changes observed in the UV−visible absorption spectrum of $Ru(bpy)_2(deeb)^{2+}$ upon iodide addition are also consistent with the above equilibrium. Following the approach of Benesi and Hildebrand, we modeled the spectral data with eq 6,

$$K = \frac{[Ru{-}I]_{eq}}{([Ru]_0 - [Ru{-}I]_{eq}) \times ([I^-]_0 - [Ru{-}I]_{eq})} \qquad (6)$$

where $[Ru]_0$ and $[I^-]_0$ are the initial molar concentrations of $Ru(bpy)_2(deeb)(PF_6)_2$ and I^-, respectively, and $[Ru{-}I]_{eq}$ is the unknown molar concentration of the $[Ru(bpy)_2(deeb),I]^+$ adduct at equilibrium.[21] Benesi and Hildebrand assumed that the equilibrium concentrations of the adduct were small relative to the concentration of added iodide, and therefore, one could substitute $[I^-]_0$ for $([I^-]_0 - [Ru{-}I]_{eq})$, simplifying eq 6 considerably. That assumption leads to a poor fit of our data as the formed Ru−I adduct is present at a concentration comparable to that of iodide. If we assume that the change in absorption observed at 365 nm upon the addition of I^- to $Ru(bpy)_2(deeb)^{2+}$ is directly proportional to the $[Ru{-}I]_{eq}$, this concentration can be calculated by eq 7:

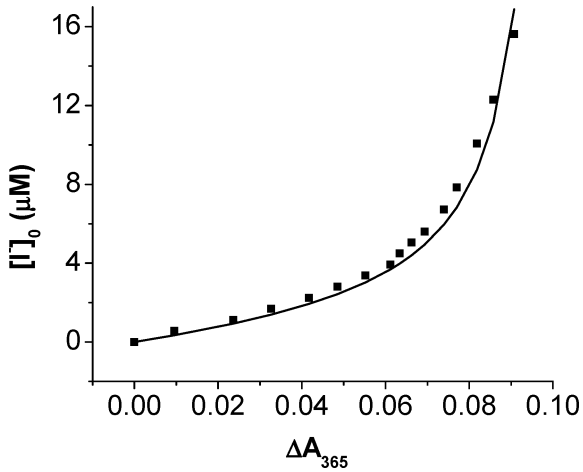

Figure 8. Plot of the initial tetrabutylammonium iodide concentration, $[I]_0$, vs the change in steady-state absorption measured at 365 nm, ΔA_{365}. Superimposed is a best-fit line generated by eq 8 with $K = 59\ 700\ M^{-1}$ and $[Ru]_0 = 18\ \mu M$. The fit yielded an extinction coefficient, $\epsilon = 5600\ M^{-1}cm^{-1}$, for the $[Ru(bpy)_2(deeb),I]^+$ ion pair at 365 nm.

$$[Ru{-}I]_{eq} = \frac{\Delta A_{365}}{\epsilon_{365}} \qquad (7)$$

where ΔA_{365} is the change in absorption at 365 nm and ϵ_{365} is the extinction coefficient of the $[Ru(bpy)_2(deeb),I]^+$ adduct. Substitution of eq 7 into eq 6, followed by rearrangement yields eq 8:

$$[I]_0 = \frac{\dfrac{\Delta A_{365}}{K \times \epsilon_{365}} - \dfrac{{\Delta A_{365}}^2}{{\epsilon_{365}}^2} + \dfrac{\Delta A_{365}}{\epsilon_{365}} \times [Ru]_0}{[Ru]_0 - \dfrac{\Delta A_{365}}{\epsilon_{365}}} \qquad (8)$$

This equation accurately modeled the steady-state absorption data, Figure 8. By fixing the equilibrium constant to the value abstracted from the static component of the time-resolved photoluminescence data and the Ru concentration to that obtained from the ground-state absorption, the extinction coefficient of the charge-transfer adduct was obtained, $\epsilon_{365} = 5600\ M^{-1}\ cm^{-1}$. Similar analysis of the absorption change upon the addition of iodide to $Ru(bpy)_3^{2+}$ resulted in $K = 14\ 500\ M^{-1}$ and $\epsilon_{375} = 3600\ M^{-1}\ cm^{-1}$.

In summary, the steady-state and time-resolved photoluminescence data and the UV−visible absorption spectra of $Ru(bpy)_2(deeb)^{2+}$ in dichloromethane with added iodide gave self-consistent values for the equilibrium constant depicted in eq 3, $K = 59\ 700\ M^{-1}$. These data, coupled with

(22) Persson, P.; Lunell, S.; Ojamae, L. *Chem. Phys. Lett.* **2002**, *364*(5−6), 469−474.
(23) Demas, J. N.; Addington, J. W. *J. Am. Chem. Soc.* **1976**, *98*(19), 5800−5806.

the fact that the static components to the time-resolved photoluminescence data and the UV−visible absorption changes are largely absent in 100 mM concentrations of inert salt, provide compelling evidence for ion-pair formation.

Iodide Oxidation. The oxidation of iodide by transition metal compounds in aqueous solution is known to occur by two parallel pathways, eqs 9 and 10.[24]

$$M_{ox} + I^- \rightarrow M_{red} + I^\bullet \quad (9)$$

$$M_{ox} + 2I^- \rightarrow M_{red} + I_2^{\bullet -} \quad (10)$$

Both reactions are first-order in the transition metal compound, but are first- and second-order in iodide concentrations. The formally third-order reaction (eq 10) has been proposed to occur by a reaction of iodide with an $M_{ox}I^-$ ion pair or of M_{ox} with an I^-,I^- ion pair[24]. Iodide oxidation by MLCT excited states has received very little attention, and neither pathway has been firmly established. Demas has reported Stern−Volmer quenching constants of $<1\ M^{-1}$ for the aqueous quenching of $Ru(bpy)_3^{2+*}$ and $Ru(bpy)_2(CN)_2^*$ by iodide.[23] The mechanism(s) for this inefficient quenching remains unknown. Balzani and others have observed efficient iodide quenching of the $Cr(bpy)_3^{2+*}$ ligand field emission but did not report the mechanism(s).[9] We note that iodide has also been widely used to promote singlet → triplet intersystem crossing in aromatic organic compounds.[8]

With such a paucity of mechanistic data on the photooxidation of iodide by Ru(II) polypyridyl compounds, we performed nanosecond transient-absorption measurements. These experiments were performed at 10 mM iodide concentrations where >99% of the excited states were quenched and the Ru(II) compounds were expected to be fully ion paired, i.e., 1:2 Ru/I adducts. Pulsed-light excitation of $[Ru(bpy)_2(deeb),(I)_2]$ showed clear evidence for a rapid reductive electron-transfer quenching mechanism. Both the reduced ruthenium compound, $Ru(bpy)_2(deeb^-)^+$, and the oxidized iodide product, $I_2^{\bullet -}$, were observed within our instrument response time. Therefore, with a rate constant greater than $10^8\ s^{-1}$, the products shown in eq 10 were spectroscopically observed. If one envisions a solution structure similar to that observed by X-ray crystallography, the close proximity of the two iodide ions may facilitate the rapid formation of $I_2^{\bullet -}$ as a result of a reaction between an iodine atom, $I^\bullet$, and the other associated iodide. Alternatively, $I_2^{\bullet -}$ could be formed by a concerted oxidation of the two iodide ions, which would be the more thermodynamically favorable pathway.[24] Precedence for the concerted formation of $I_2^{\bullet -}$ can be found in the work of Mialocq and co-workers, who have shown that excitation into an iodide → viologen charge-transfer band resulted in the subpicosecond formation of singly reduced viologen and $I_2^{\bullet -}$. Quantum mechanical calculations showed that the concerted pathway could occur when the iodide ions were within 4−8 Å of each other.[25] Although these distances are well within that measured crystallographically for $Ru(bpy)_2(deeb)(I)_2$, further experiments on shorter time scales are required to firmly establish the mechanism.

Scheme 1

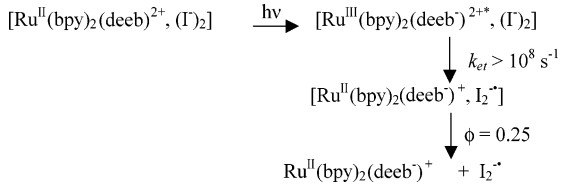

The quantum yields for $I_2^{\bullet -}$ were found to be 0.25 with 355 or 532 nm excitation. Because >99% of the excited states were quenched under the conditions of the experiments, we attribute this to the cage-escape yield. Interestingly, the yield increased to 0.50 after the excitation of $Ru(bpy)_3^{2+}$ in concentrated iodide solutions. The higher yield may result from a weaker adduct with $I_2^{\bullet -}$ that allows a greater fraction of the products to escape the solvent cage. Recall that the equilibrium constants with iodide are about a factor of 4 smaller for $Ru(bpy)_3^{2+}$ than those for $Ru(bpy)_2(deeb)^{2+}$.

The photophysical results can thus be summarized as shown in Scheme 1. Photoexcitation of $[Ru(bpy)_2(deeb),(I)_2]$ results in the oxidation of iodide to form $I_2^{\bullet -}$ and the reduced complex, $Ru^{II}(bpy)_2(deeb^-)^+$, with a rate constant $>10^8\ s^{-1}$. These products escape the solvent cage to yield charge-separated products with a quantum yield of 0.25. The behavior is similar for $Ru(bpy)_3^{2+*}$, but the cage-escape yield is a factor of 2 higher. The fate of the charge-separated products is not completely clear from these experimental studies.

In bimolecular reductive electron-transfer studies, charge-separated products were expected to return to ground-state products with second-order equal-concentration kinetics. This was not the case for $Ru^{II}(bpy)_2(deeb^-)^+$ and $I_2^{\bullet -}$. The concentration of $Ru(bpy)_2(deeb^-)^+$ decreased with single-exponential kinetics, $k = 1.15 \times 10^5\ s^{-1}$. On the other hand, the $I_2^{\bullet -}$ concentration decreased with second-order kinetics, $k = 7 \times 10^9\ M^{-1}\ s^{-1}$. Both $Ru^{II}(bpy)_2(deeb^-)^+$ and $I_2^{\bullet -}$ returned cleanly to baseline without the appearance of any new absorption features. This indicates that they either form ground-state products or form intermediates that do not absorb light appreciably in the 400−800 nm region.

A clear explanation for the differing kinetic rate constants and reaction orders for the two photoproducts is not known. An initial idea was that $Ru(bpy)_2(deeb^-)^+$ reacts in dichloromethane in a manner similar to that known for MLCT excited states. Van Houten has shown that $Ru(bpy)_3^{2+*}$ reacts in CH_2Cl_2 to yield *cis*-$Ru(bpy)_2Cl_2$ in high yield.[26] We have not observed spectroscopic evidence for Ru(II) dihalo products or for solvent photochemistry by GC−MS. In fact, ion pairing with iodide suppresses the photochemistry reported by Van Houten, and upon prolonged photolysis, the only product observed was tri-iodide. The second-order rate constant for $I_2^{\bullet -}$ loss was $7 \times 10^9\ M^{-1}\ s^{-1}$, which is quite close to the reported disproportionation rate constant in

(24) Nord, G. *Comm. Inorg. Chem.* **1992**, *13*, 221−239.
(25) Jarzeba, W.; Pommeret, S.; Mialocq, J. C. *Chem. Phys. Lett.* **2001**, *333*(6), 419−426.
(26) Jones, W. E.; Smith, R. A.; Abramo, M. T.; Williams, M. D.; Vanhouten, J. *Inorg. Chem.* **1989**, *28*(12), 2281−2285.

aqueous solution.[27] Disproportionation is known to yield iodide and tri-iodide.[27] We have shown that the lifetime of $Ru^{II}(bpy)_2(deeb^-)^+$ is quenched by I_3^- with a rate constant of 2.2×10^{10} M^{-1} s^{-1}. On the basis of these data, our preliminary hypothesis is that the $I_2^{\bullet -}$ disproportionates to yield tri-iodide and iodide. The tri-iodide product is reduced by $Ru^{II}(bpy)_2(deeb^-)^+$.

Conclusions

We have demonstrated a static electron-transfer quenching mechanism for iodide photooxidation with visible light. The process is initiated by MLCT light excitation of Ru(II) bipyridyl compounds ion paired with iodide. For micromolar concentrations in dichloromethane, a 1:1 Ru(II)/I^- stoichiometry is achieved with an equilibrium constant $K = 59\,700$ M^{-1}. The spectroscopic data strongly suggest that the Ru(II)−iodide adducts arise from interactions between iodide and the diimine ligand(s) as well as ion pairing. At higher iodide concentrations, there was evidence for a 1:2 Ru(II)/I^- stoichiometry. Pulsed-light excitation of the $[Ru(bpy)_2(deeb),(I)_2]$ ion pair in dichloromethane ultimately yielded $Ru(bpy)_2(deeb^-)^+$ and $I_2^{\bullet -}$ charge-separated states with quantum yields of 0.25. Thus, for solar energy conversion applications, a green photon can store ∼1.7 eV of free energy for tens of microseconds.

Sensitizer−iodide interactions may be relevant to dye-sensitized solar cells, particularly in solid-state embodiments.[28] Our ability to observe ion pairing in relatively polar solvents (such as acetonitrile) and at millimolar ionic strengths suggests that ion pairing may even be more general.[5−7,19] Indeed, in the course of this work, a literature report of iodide oxidation by a photoexcited, TiO_2-bound Ru(II) sensitizer was reported.[29] Thus, iodide oxidation *can* compete with ultrafast electron injection into TiO_2 under some conditions. Excited-state iodide oxidation need not lower the solar-cell efficiency, provided that the reduced sensitizers quantitatively inject electrons into the semiconductor.[30,31] Studies of this type are now underway in our laboratories.

Acknowledgment. The Division of Chemical Sciences, Office of Basic Energy Sciences, Office of Energy Research, U.S. Department of Energy are gratefully acknowledged for research support.

Supporting Information Available: Crystallographic data of $Ru(bpy)_2(deeb)(I)_2$ in CIF format. This material is available free of charge via the Internet at http://pubs.acs.org.

IC051467J

(27) Grossweiner, L. I.; Matheson, M. S. *J. Phys. Chem.* **1957**, *61*(8), 1089−1095.

(28) Bach, U.; Lupo, D.; Comte, P.; Moser, J. E.; Weissortel, F.; Salbeck, J.; Spreitzer, H.; Gratzel, M. *Nature* **1998**, *395*(6702), 583−585.

(29) Wang, P.; Wenger, B.; Humphry-Baker, R.; Moser, J. E.; Teuscher, J.; Kantlehner, W.; Mezger, J.; Stoyanov, E. V.; Zakeeruddin, S. M.; Gratzel, M. *J. Am. Chem. Soc.* **2005**, *127*, 6850−6856.

(30) Thompson, D. W.; Kelly, C. A.; Farzad, F.; Meyer, G. J. *Langmuir* **1999**, *15*, 650.

(31) Ortmans, I.; Moucheron, C.; Kirsch De MesMaker, A. *Coord. Chem. Rev.* **1998** *168*, 233 and references therein.